Vìsnik Dnìpropetrovs'kogo unìversitetu. Serìâ hìmìâ 23 (2015), 2, 1–9

Вісник Дніпропетровського університету. Серія хімія

Bulletin of Dnipropetrovsk University. Series Chemistry

p-ISSN 2306-871X, e-ISSN 2313-4984
journal homepage: http://chemistry.dnu.dp.ua

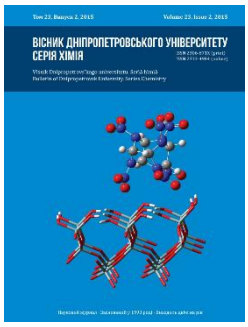

UDC 544.431.24

STRUCTURE AND REDOX PROPERTIES OF 2,4,6,8,10,12-HEXANITRO-2,4,6,8,10,12-HEXAAZAISOWURTZITANE (CL-20) ADSORBED ON A SILICA SURFACE. M05 COMPUTATIONAL STUDY

Liudmyla K. Sviatenko*,[1] Leonid Gorb,[2] Sergiy I. Okovytyy[1]
[1]*Oles Honchar Dnipropetrovsk National University, 72 Gagarin Ave., Dnipropetrovsk 49010, Ukraine*
[2]*HX5, LLC, Vicksburg, Mississippi 39180, USA*
Received 30 October 2015; revised 10 December 2015; accepted 12 December 2015, available online 17 March 2016

Abstract

The cluster approximation was applied at M05/tzvp level to model adsorption of 2,4,6,8,10,12-hexanitro-2,4,6,8,10,12-hexaazaisowurtzitane (CL-20) on (001) surface of α-quartz. Structures of the obtained CL-20–silica complexes confirm close to parallel orientation of the nitrocompound toward surface. The binding between CL-20 and silica surface was analyzed and bond energies were calculated applying the atoms in molecules (AIM) method. Hydrogen bonds were found to significantly contribute in adsorption energy. An attaching of electron leads to significant deviation from coplanarity in complexes and to strengthening of hydrogen bonding. Redox properties of adsorbed CL-20 were compared with those of gas-phase and hydrated species by calculation of electron affinity, ionization potential, reduction Gibbs free energy, oxidation Gibbs free energy, reduction and oxidation potentials. It was shown that adsorbed CL-20 has lower ability to redox transformation as compared with hydrated one.

Keywords: silica; adsorption; reduction; oxidation; CL-20.

СТРУКТУРА І ОКИСЛЮВАЛЬНО-ВІДНОВНІ ВЛАСТИВОСТІ 2,4,6,8,10,12-ГЕКСАНІТРО-2,4,6,8,10,12-ГЕКСААЗАІЗОВЮРЦІТАНА (CL-20), АДСОРБОВАНОГО НА ПОВЕРХНІ КВАРЦУ. M05 РОЗРАХУНКОВЕ ДОСЛІДЖЕННЯ

Людмила К. Святенко*,[1] Леонід Горб,[2] Сергій І. Оковитий[1]
[1]*Дніпропетровський національний університет імені Олеся Гончара, просп. Гагаріна, 72, Дніпропетровськ 49010, Україна*
[2]*HX5, LLC, Віксбург, Міссісіпі 39180, США*

Анотація

Адсорбція 2,4,6,8,10,12-гексанітро-2,4,6,8,10,12-гексаазаізовюрцітана (CL-20) на (001) поверхні альфа-кварцу змодельована в кластерному наближенні на M05 теоретичному рівні. Структури отриманих комплексів CL-20–кварц підтверджують близьку до паралельної орієнтацію нітросполуки до поверхні. Методом AIM проведено аналіз зв'язування між CL-20 і поверхнею кварцу і розраховані енергії зв'язку. Виявлено, що водневі зв'язки вносять значний вклад в енергії адсорбції. Приєднання електрона призводить до значного відхилення від компланарності в комплексах і посиленню водневих зв'язків. Окислювально-відновні властивості адсорбованого, газофазного і гідратованого CL-20 порівняні між собою шляхом аналізу розрахованих спорідненості до електрона, потенціалу іонізації, вільної енергії Гіббса відновлення та окислення, потенціалів відновлення та окислення. Показано, що адсорбований CL-20 має більш низьку здатність до редокс-перетворень у порівнянні з гідратованим.

Ключові слова: кварц; адсорбція; відновлення; окислення; CL-20.

**Correspoding author: tel.: +380667892140; e-mail address: lsv@icnanotox.org*

doi: 10.15421/081511

Vìsnik Dnìpropetrovs'kogo unìversitetu. Serìâ hìmìâ 23 (2015), 2, 1–9

СТРУКТУРА И ОКИСЛИТЕЛЬНО-ВОССТАНОВИТЕЛЬНЫЕ СВОЙСТВА 2,4,6,8,10,12-ГЕКСАНИТРО-2,4,6,8,10,12-ГЕКСААЗАИЗОВЮРЦИТАНА (CL-20), АДСОРБИРОВАННОГО НА ПОВЕРХНОСТИ КВАРЦА. M05 РАСЧЕТНОЕ ИССЛЕДОВАНИЕ

Людмила К. Святенко*,[1] Леонид Горб,[2] Сергей И. Оковитый[1]

[1]*Днепропетровский национальный университет имени Олеся Гончара, просп. Гагарина, 72, Днепропетровск 49010, Украина*

[2]*HX5, LLC, Виксбург, Миссисипи 39180, США*

Аннотация

Адсорбция 2,4,6,8,10,12-гексанитро-2,4,6,8,10,12-гексаазаизовюрцитана (CL-20) на (001) поверхности альфа-кварца смоделирована в кластерном приближении на M05 теоретическом уровне. Структуры полученных комплексов CL-20–кварц подтверждают близкую к параллельной ориентацию нитросоединения к поверхности. Методом AIM проведен анализ связывания между CL-20 и поверхностью кварца и рассчитаны энергии связи. Обнаружено, что водородные связи вносят значительный вклад в энергии адсорбции. Присоединение электрона приводит к значительному отклонению от компланарности в комплексах и усилению водородных связей. Окислительно-восстановительные свойства адсорбированного, газофазного и гидратированного CL-20 сравнены между собой путем анализа рассчитанных сродства к электрону, потенциала ионизации, свободной энергии Гиббса восстановления и окисления, потенциалов восстановления и окисления. Показано, что адсорбированный CL-20 имеет более низкую способность к редокс-преобразованиям по сравнению с гидратированным.

Ключевые слова: кварц; адсорбция; восстановление; окисление; CL-20.

Introduction

Sorption of organic chemicals to soil is a major process that can affect their mobility, degradation and toxicity by reducing their availability. A fundamental understanding of sorption and desorption mechanisms is therefore essential for the accurate prediction of the fate and impact of organic contaminants in soils and groundwater. Recently redox properties of such nitro-compounds as **2,4-dinitroanisole (DNAN)**, **2,4-dinitrotoluene (DNT)**, **trinitrotoluene (TNT)**, and **5-nitro-2,4-dihydro-3H-1,2,4-triazol-3-one (NTO)**, **5-amino-3-nitro-1H-1,2,4-triazole (ANTA)** adsorbed to silica, as a model for soil components, and dissolved in water have been investigated [1; 2]. It was shown that adsorbed nitrocompounds are hardier to transform by oxidation or reduction than their dissolved in water counterparts. In this study, we extended investigation of redox properties of nitrocompounds under different environmental conditions to include polycyclic nitramine **2,4,6,8,10,12-hexanitro-2,4,6,8,10,12-hexa-aza-isowurtzitane (CL-20)**, which is a high-density energetic material. **CL-20** could be dispersed in the environment during production, processing, destruction, and recycling. It was found to be toxic to soil invertebrates and some aquatic organisms [3; 4] thereby its removal from contaminated environments is an actual and important task. Study of **CL-20** interactions with soil will help understand and predict the fate and environmental impact of this powerful energetic compound.

Computational Methodology

All of the calculations were performed using the Gaussian 09 program package [5]. The geometry of neutral, cation- and anion-radical species were optimized using the Density Functional Theory at the M05/tzvp level [6; 7]. The present functional and basis set were chosen because of the results of our recent study where such level of theory was able to provide accuracy close to that obtained by experimental measurements [8]. Cluster approach to simulate the hydroxylated (001) surface for α-quartz has been utilized [9]. In order to keep the silica model electroneutral, dangling bonds of the cluster were saturated by hydrogen atoms (for clarity only hydrogen atoms saturating dangling bonds on the top of silica surface models are shown in the Figures). This method for termination of the missing bonds has been shown to be the one of most efficient in theoretical studies on the adsorption of different organic molecules on silicate minerals [10]. The models obtained contain six oxygen-silicon-oxygen layers, with a formula of $Si_{44}O_{118}H_{60}$. Harmonic vibrational frequencies were calculated for all structures obtained, to establish that a minimum was observed. Adsorption energy was calculated as a difference between the total energy of the adsorbed complex and the energy of the separated silica and **CL-20**, corrected for basis set superposition error using the counterpoise method.

The topological analysis of the distribution function of the electron density $\rho(r)$ was carried

out for the optimized geometry of the complexes in the framework of the R. Bader *atoms in molecules* (AIM) theory [11] using the Multiwfn program [12]. Binding energy of interactions (E) calculated with the Espinosa formula E=0.5·V, where V is the density of potential energy in critical point.

Adiabatic electron affinities (E_A) and ionization potentials (I_p) were calculated as the total energy difference between charged species and neutral forms, corrected for zero point energy. The Gibbs free energies of electron transfer for **CL-20** under dissolution and under adsorption were calculated as follows:

i) water hydration:

$$\Delta G^0_{red,solv} = \Delta G^0(R^{-\cdot}_{solv}) - \Delta G^0(O_{solv})$$
$$\Delta G^0_{ox,solv} = \Delta G^0(O^{+\cdot}_{solv}) - \Delta G^0(R_{solv}) \quad (1)$$

ii) α-quartz adsorption:

$$\Delta G^0_{red,ads} = \Delta G^0(R^{-\cdot}_{ads}) - \Delta G^0(O_{ads})$$
$$\Delta G^0_{ox,ads} = \Delta G^0(O^{+\cdot}_{ads}) - \Delta G^0(R_{ads}) \quad (2)$$

The values of reduction and oxidation potentials are expressed as

$$E^0_{red} = -\frac{\Delta G^0_{red}}{nF} + E_H$$
$$E^0_{ox} = \frac{\Delta G^0_{ox}}{nF} + E_H \quad (3)$$

The absolute potential of the NHE reference electrode E_H is taken as –4.36 eV. The solvent effects were assessed by single-point calculations using a PCM (Pauling) and SMD solvation models for ion-radical and neutral molecule calculations, respectively [13; 14].

Results and Discussion

Adsorbed complexes

There are several conformers of **CL-20**. Based on the reported MBPT(2)/6-311G(d,p) and B3LYP/6-31G+(d,p) calculated data the most stable one, which is β conformer, was chosen for the present study (Fig. 1) [15; 16]. To search structures of adsorbed CL-20-silica complexes molecule of the nitrocompound was attached to the surface by its top (CH–CH bridge), bottom (six-membered cycle), and sides (five- and seven-membered cycles). Optimization of several complexes with different orientation of **CL-20** related to silica matrix resulted in four stable clusters **CL-20(a)$_{ads}$**, **CL-20(b)$_{ads}$**, **CL-20(c)$_{ads}$**, and **CL-20(d)$_{ads}$** with adsorption energy of –8.11, –11.00, –9.12, and –6.82 kcal/mol, respectively. The most stable one corresponds to six-membered cycle orientation of **CL-20** toward silica surface (Fig. 2). Adsorption of **CL-20** on silica surface occurs through the formation of O···H–O and O···H–C bonds (Fig. 2). These hydrogen bonds are formed between oxygen atoms of nitro-group of **CL-20** molecule (proton acceptors) and hydrogen atoms of the surface hydroxyl groups, and between the oxygen atoms of the surface (proton acceptors) and methine hydrogens of the nitrocompound.

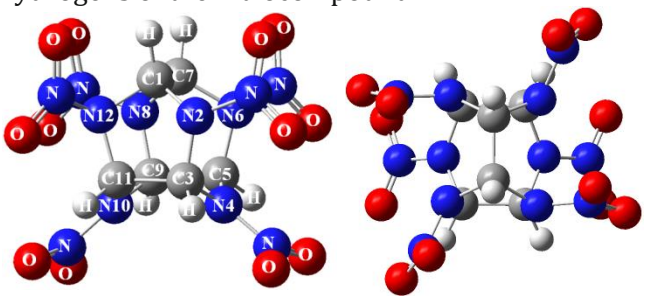

a b

Fig. 1. Structure of β-CL-20 (a – front view, b – top view)

Analysis of the data presented in Fig. 2 and Table 1 enable us to conclude that after losing or attaching an electron, there is no significant change in total orientation of nitrocompound. The most important changes are observed in the hydrogen bond distances after the electron attachment occurs. Nitrocompound was observed to orient closer to the surface by its nitro-groups. Thus, O···H–O bonds lengths decrease and their strengths increase. In contrast, an electron detachment did not cause any significant change in hydrogen bond distances.

To provide deeper insight into the nature of intermolecular interactions in complexes of **CL-20** with silica surface, the analysis of their electron density was carried out. The topological analysis of the electron density shows the presence of intermolecular bond critical points (BCPs) between the hydrogens of CH group and the closest oxygen atoms of surface (C–H···O), and between the oxygen of nitro-group and the closest hydrogen atoms of surface (O···H–O) (Tables 2–5). Decrease of distance between interacting atoms good exponentially correlates with the increase of electron density at BCPs with a correlation coefficient of 0.93 (Fig. 3). There is also good correlation between interaction energy and electron density at BCPs with a correlation coefficient of 0.98 (Fig. 3). Similar dependencies were observed earlier for different types of hydrogen bonds [17].

The calculated electron density properties of studied complexes show that interactions between **CL-20** and surface have low electron density ρ and positive Laplacian $\nabla^2\rho > 0$) (Tables 2–5). These values indicate that C–H···O and O···H–O contacts may be classified as the closed-shell interactions in which electronic charge is concentrated towards nucleus and is depleted in

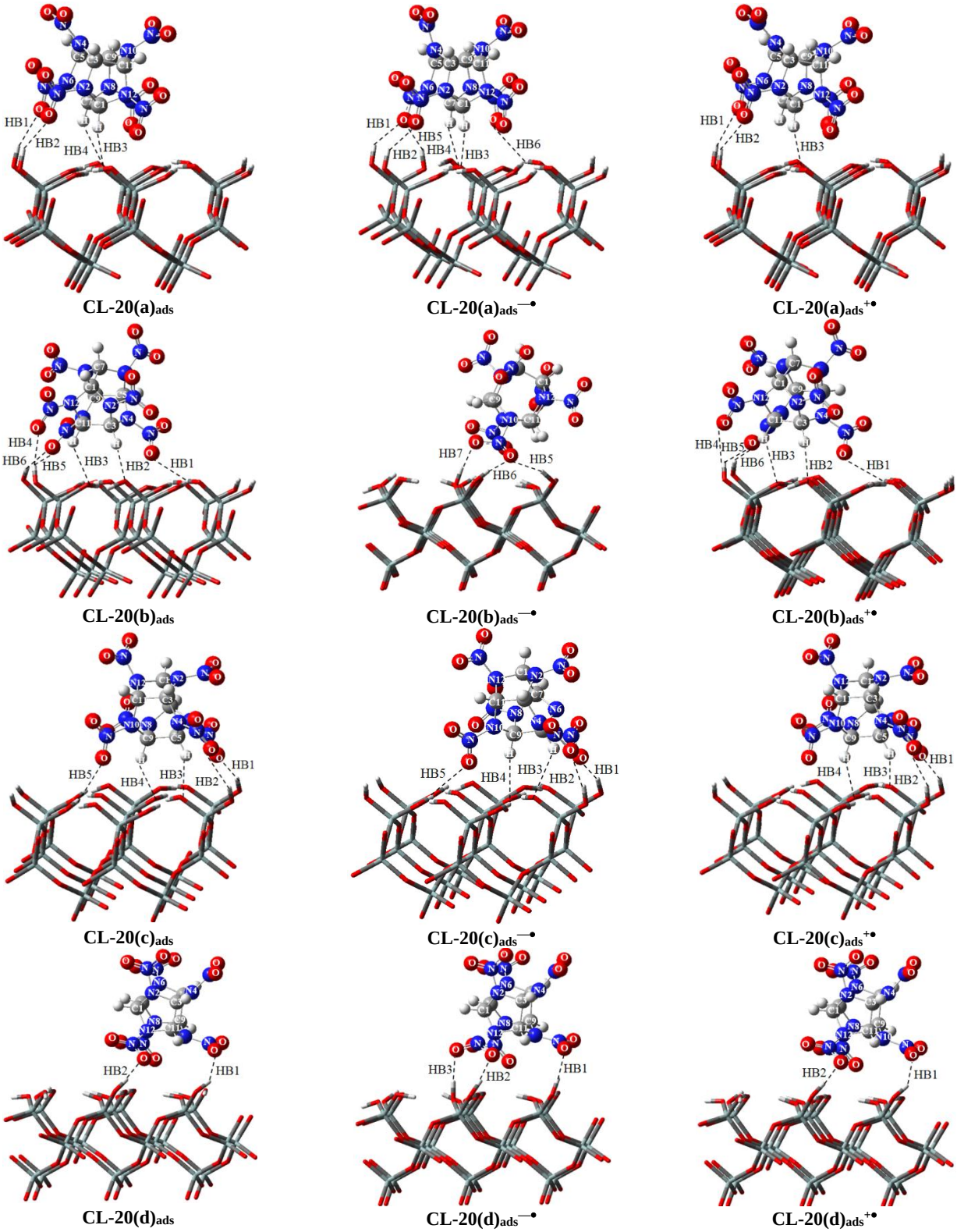

Fig. 2. The optimized structures of CL-20 adsorbed on a model of the (001) α-quartz surface and intermolecular H-bonds. Hydrogen atoms of dangling bonds are not shown

the internuclear region [18; 19]. Positive electron energy density values (H>0) indicate on noncovalent interactions, while negative H values mean that these interactions are partly covalent. Calculated topological characteristic are similar to those reported for C–H···O and O···H–O hydrogen bonds [20; 21]. Binding energy of interactions (E) calculated with the Espinosa formula ranges from –0.63 kcal/mol to –14.43 kcal/mol. Energy values show that electron attachment increases binding of the nitrocompound to the surface significantly while electron losing has negligible effect on binding energies. It should be noted that an one hydrogen bond in each anion-radical complex has

Table 1

M05/tzvp level calculated geometrical characteristics of adsorbate-adsorbent H-bonds including H···Y, X···Y distances (Å) and X–H···Y angles (degree) for adsorbed CL-20, its anion- and cation-radicals.

Bond	Bond type	X···H	X···Y	XHY	X···H	X···Y	XHY	X···H	X···Y	XHY
		CL-20(a)$_{ads}$			**CL-20(a)$_{ads}^{-\bullet}$**			**CL-20(a)$_{ads}^{+\bullet}$**		
HB1	(N6N–)O(1)···H–O	2.18	3.09	158.0	2.10	2.90	139.6	2.18	3.06	152.8
HB2	(N2N–)O···H–O	2.27	3.14	151.7	2.17	3.02	147.2	2.21	3.09	150.7
HB3	C1–H··· O	2.24	3.12	136.8	2.44	3.27	132.4	2.27	3.12	138.6
HB4	C7–H··· O	2.71	3.36	118.1	2.51	3.33	131.3	–	–	–
HB5	(N6N–)O(2)···H–O	–	–	–	1.79	2.72	157.5	–	–	–
HB6	(N8N–)O···H–O	–	–	–	2.64	3.18	115.5	–	–	–
		CL-20(b)$_{ads}$			**CL-20(b)$_{ads}^{-\bullet}$**			**CL-20(b)$_{ads}^{+\bullet}$**		
HB1	(N4N–)O···H–O	2.45	2.93	110.5	–	–	–	2.47	2.95	110.5
HB2	C3–H··· O	2.50	3.56	165.3	–	–	–	2.51	3.57	165.2
HB3	C11–H··· O	2.36	3.21	134.0	–	–	–	2.46	3.28	131.4
HB4	(N12N–)O···H–O	2.30	3.00	129.0	–	–	–	2.41	3.02	121.1
HB5	(N10N–)O···H–O(1)	2.52	3.21	129.8	1.96	2.88	157.3	2.49	3.21	132.0
HB6	(N10N–)O···H–O(2)	2.53	3.44	157.3	1.97	2.92	164.6	2.53	3.43	156.6
HB7	(N10N–)O···H–O(3)	–	–	–	1.69	2.67	168.1	–	–	–
		CL-20(c)$_{ads}$			**CL-20(c)$_{ads}^{-\bullet}$**			**CL-20(c)$_{ads}^{+\bullet}$**		
HB1	(N6N–)O···H–O	2.18	3.10	159.7	1.84	2.79	162.9	2.09	3.01	160.2
HB2	(N4N–)O···H–O	2.24	3.00	135.3	2.04	2.99	168.5	2.11	3.00	155.6
HB3	C5–H··· O	2.24	3.20	145.9	2.67	3.44	127.0	2.44	3.33	137.7
HB4	C9–H··· O	2.45	3.37	141.5	2.58	3.64	166.7	2.41	3.34	142.7
HB5	(N10N–)O···H–O	2.64	3.26	122.5	2.71	3.26	124.9	–	–	–
		CL-20(d)$_{ads}$			**CL-20(d)$_{ads}^{-\bullet}$**			**CL-20(d)$_{ads}^{+\bullet}$**		
HB1	(N10N–)O···H–O	2.22	3.01	139.5	1.96	2.91	169.9	2.02	2.93	157.2
HB2	(N12N–)O(1)···H–O	2.40	3.29	154.2	1.93	2.88	166.1	2.33	3.24	157.5
HB3	(N12N–)O(2)···H–O	–	–	–	1.78	2.75	172.1	–	–	–

Table 2

Topological parameters for adsorbed CL-20(a), its anion- and cation-radical

Bond	Bond type	ρ, $e{\cdot}Å^{-3}$	$\nabla^2\rho$, $e{\cdot}Å^{-5}$	*H*, au	*E*, kcal/mol
	CL-20(a)$_{ads}$				
HB1	(N6N–)O(1)···H–O	0.0107	0.0528	0.0030	–2.26
HB2	(N2N–)O···H–O	0.0096	0.0443	0.0026	–1.85
HB3	C1–H··· O	0.0144	0.0588	0.0027	–2.95
HB4	C7–H··· O	0.0058	0.0254	0.0014	–1.10
	CL-20(a)$_{ads}^{-\bullet}$				
HB1	(N6N–)O(1)···H–O	0.0164	0.0699	0.0028	–3.77
HB2	(N2N–)O···H–O	0.0131	0.0581	0.0029	–2.73
HB3	C1–H··· O	0.0093	0.0384	0.0021	–1.73
HB4	C7–H··· O	0.0085	0.0340	0.0017	–1.60
HB5	(N6N–)O(2)···H–O	0.0346	0.1137	–0.0022	–10.26
HB6	(N8N–)O···H–O	0.0050	0.0247	0.0016	–0.91
	CL-20(a)$_{ads}^{+\bullet}$				
HB1	(N6N–)O(1)···H–O	0.0110	0.0542	0.0030	–2.35
HB2	(N2N–)O···H–O	0.0110	0.0507	0.0028	–2.20
HB3	C1–H··· O	0.0147	0.0601	0.0027	–3.04
HB4	C7–H··· O	0.0048	0.0174	0.0010	–0.75

negative H value and, correspondently, the biggest energy. All BCPs of neutral and cation-radical complexes are characterized by positive H values.

Redox properties

Electron affinity, Gibbs free energy of reduction, and reduction potential were calculated to characterize ability of **CL-20** to be reduced (Table 6), while ability of CL-20 to oxidation is reflected by ionization energy, Gibbs free energy of oxidation, and oxidation potential (Table 7). The abovementioned parameters were calculated for **CL-20** located in gas phase, adsorbed by silica surface, and dissolved in aqueous solution. The data presented in Tables 6 and 7 show that the ability of the nitramine to attach or to lose an electron significantly depends from its surrounding and increases in the row gas<adsorbed species<hydrated form. This means that hydration more contribute to Gibbs free energy of electron transfer as compared with adsorption, i.e. energy difference between hydration of ion-radical and neutral molecule is larger than that between corresponding adsorbed species. As a result, adsorbed species will be more resistant to redox transformations than hydrated ones. The similar trend was observed by us earlier for **TNT**, **DNT**, **DNAN**, **NTO** and **ANTA** [1; 2]. Electron attachment more reduces gas-phase Gibbs free energies (0.7–1.1 eV) than electron lose (0.5–0.9 eV) for adsorbed species (Tables 6, 7).

Table 3

Topological parameters for adsorbed CL-20(b), its anion- and cation-radical

Bond	Bond type	ρ, *e*·*Å*$^{-3}$	∇^{2}ρ, *e*·*Å*$^{-5}$	*H*, au	*E*, kcal/mol
	CL-20(b)$_{ads}$				
HB1	(N4N–)O···H–O	0.0085	0.0453	0.0028	–1.79
HB2	C3–H··· O	0.0074	0.0290	0.0017	–1.19
HB3	C11–H··· O	0.0116	0.0450	0.0022	–2.13
HB4	(N12N–)O···H–O	0.0093	0.0472	0.0028	–1.98
HB5	(N10N–)O···H–O(1)	0.0063	0.0290	0.0018	–1.16
HB6	(N10N–)O···H–O(2)	0.0059	0.0233	0.0015	–0.91
	CL-20(b)$_{ads}^{-\bullet}$				
HB5	(N10N–)O···H–O(1)	0.0236	0.0844	0.0013	–5.80
HB6	(N10N–)O···H–O(2)	0.0232	0.0806	0.0013	–5.52
HB7	(N10N–)O···H–O(3)	0.0451	0.1274	–0.0071	–14.43
	CL-20(b)$_{ads}^{+\bullet}$				
HB1	(N4N–)O···H–O	0.0082	0.0433	0.0027	–1.69
HB2	C3–H··· O	0.0073	0.0284	0.0017	–1.16
HB3	C11–H··· O	0.0095	0.0366	0.0019	–1.69
HB4	(N12N–)O···H–O	0.0077	0.0393	0.0024	–1.57
HB5	(N10N–)O···H–O(1)	0.0066	0.0301	0.0018	–1.22
HB6	(N10N–)O···H–O(2)	0.0060	0.0239	0.0015	–0.94

Table 4

Topological parameters for adsorbed CL-20(c), its anion- and cation-radical

Bond	Bond type	ρ, *e*·*Å*$^{-3}$	∇^{2}ρ, *e*·*Å*$^{-5}$	*H*, au	*E*, kcal/mol
	CL-20(c)$_{ads}$				
HB1	(N6N–)O···H–O	0.0130	0.0553	0.0029	–2.54
HB2	(N4N–)O···H–O	0.0099	0.0506	0.0028	–2.16
HB3	C5–H··· O	0.0144	0.0558	0.0025	–2.79
HB4	C9–H··· O	0.0093	0.0359	0.0019	–1.63
HB5	(N10N–)O···H–O	0.0040	0.0205	0.0014	–0.72
	CL-20(c)$_{ads}^{-\bullet}$				
HB1	(N6N–)O···H–O	0.0307	0.0995	–0.0010	–8.47
HB2	(N4N–)O···H–O	0.0148	0.0713	0.0033	–3.51
HB3	C5–H··· O	0.0065	0.0024	0.0013	–1.13
HB4	C9–H··· O	0.0066	0.0248	0.0014	–1.07
HB5	(N10N–)O···H–O	0.0038	0.0176	0.0012	–0.63
	CL-20(c)$_{ads}^{+\bullet}$				
HB1	(N6N–)O···H–O	0.0160	0.0679	0.0030	–3.48
HB2	(N4N–)O···H–O	0.0128	0.0636	0.0033	–2.92
HB3	C5–H··· O	0.0095	0.0366	0.0019	–1.66
HB4	C9–H··· O	0.0099	0.0389	0.0021	–1.76

Table 5

Topological parameters for adsorbed CL-20(d), its anion- and cation-radical

Bond	Bond type	ρ, *e*·*Å*$^{-3}$	∇^{2}ρ, *e*·*Å*$^{-5}$	*H*, au	*E*, kcal/mol
	CL-20(d)$_{ads}$				
HB1	(N10N–)O···H–O	0.0113	0.0538	0.0029	–2.45
HB2	(N12N–)O(1)···H–O	0.0078	0.0333	0.0021	–1.32
	CL-20(d)$_{ads}^{-\bullet}$				
HB1	(N10N–)O···H–O	0.0198	0.0843	0.0026	–4.96
HB2	(N12N–)O(1)···H–O	0.0254	0.0871	0.0008	–6.34
HB3	(N12N–)O(2)···H–O	0.0364	0.1083	–0.0033	–10.57
	CL-20(d)$_{ads}^{+\bullet}$				
HB1	(N10N–)O···H–O	0.0173	0.0773	0.0030	–4.17
HB2	(N12N–)O(1)···H–O	0.0088	0.0383	0.0023	–1.54

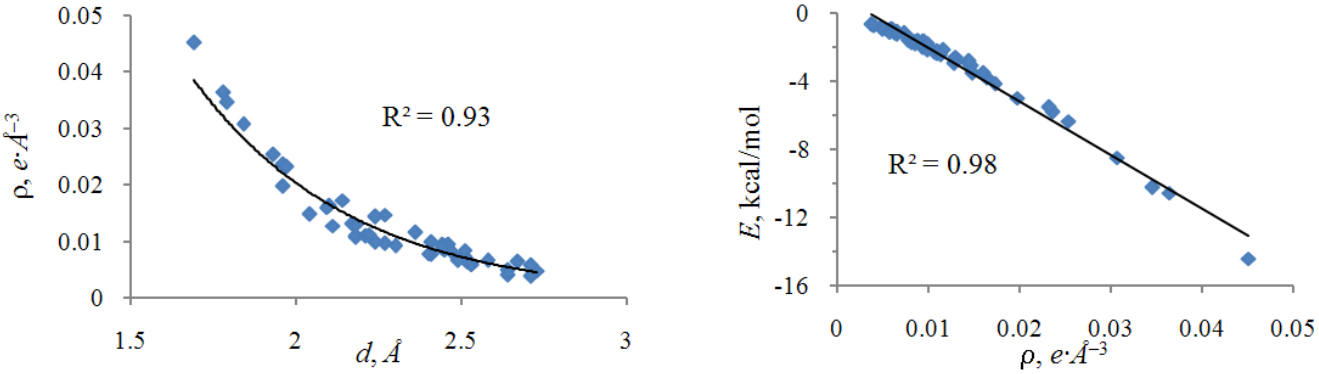

Fig. 3. Plots of (a) electron density at BCP *vs.* bond distance, (b) interaction energy *vs.* electron density at BCP for studied complexes (N=50)

Table 6

M05/tzvp and SMD/PCM (Pauling)/M05/tzvp levels calculated electron affinities, Gibbs free energies of reduction, and reduction potentials of CL-20

Compound	E_A, eV			ΔG^0_{red}, eV			E^0_{red}, eV	
	gas	ads	water	gas	ads	water	ads	water
CL-20(a)		−2.53			−2.63		−1.73	
CL-20(b)	−1.60	−2.30	−3.95	−1.60	−2.41	−3.88	−1.95	−0.48
CL-20(c)		−2.18			−2.29		−2.07	(−0.39 [24])
CL-20(d)		−2.61			−2.73		−1.63	

Table 7

M05/tzvp and SMD/PCM (Pauling)/M05/tzvp levels calculated ionization energies, Gibbs free energies of oxidation, and oxidation potentials of CL-20

Compound	I_p, eV			ΔG^0_{ox}, eV			E^0_{ox}, eV	
	gas	ads	water	gas	ads	water	ads	water
CL-20(a)		8.73			8.63		4.27	
CL-20(b)	9.30	8.95	4.94	9.30	8.84	4.99	4.48	0.63
CL-20(c)		8.85			8.73		4.37	
CL-20(d)		8.80			8.71		4.35	

This means that anion-radicals more strongly bind to the silica surface than corresponding cation-radicals that is confirmed by calculated binding energies (Tables 2–5). In contrast, hydration is stronger for cation-radical of **CL-20** than for its anion-radical that is reflected by larger decrease of electron detachment Gibbs free energy (4.3 eV) than electron capture Gibbs free energy (2.3 eV).

According to Pourbaix diagram of an iron/water system [22] the Fe(II)/Fe(III) couple and metallic iron are not able to reduce **CL-20** under natural conditions at neutral pH (Fig. 4). Experimental evidence completely suggests calculated data indicating that Fe^0 and dissolved Fe^{2+} ions were not responsible for the degradation of **CL-20** [23]. It should be noted that as in line with our previous study of redox properties of adsorbed nitrocompounds we expect the values of reduction potential for adsorbed **CL-20** to be more negative than value for solvated one just by 0.1–0.2 eV because hydration of the contaminant, typical in its adsorption by soil under natural conditions, was not included in calculation of adsorbed redox potentials [1]. In alkaline conditions (pH>9) iron (II) hydroxide is capable to reduce **CL-20**, while mixed iron (II, III) oxide provides sufficient reducing potential for **CL-20** at very high pH>11. Reduction of **CL-20** under natural conditions may be performed, for instance, by surface-bound Fe^{2+}.

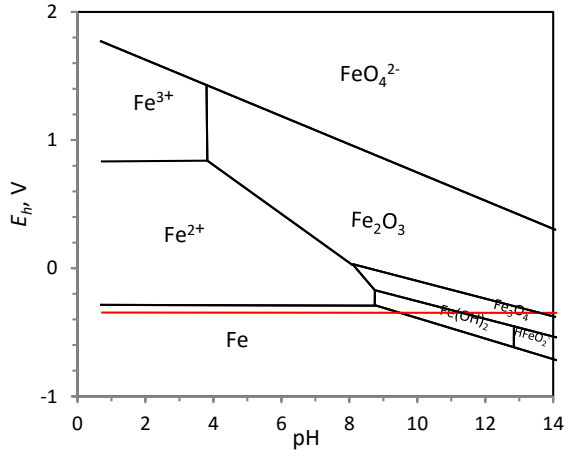

Fig. 4. Pourbaix diagram for an iron-water system at 298 K and 1 atm. Red horizontal lines mark CL-20

Conclusions

Structures of complexes formed due to adsorption of **CL-20** on (001) surface of α-quartz were modeled at M05/tzvp level. **CL-20** binds with surface by C–H···O and O···H–O hydrogen bonds, which accordingly to topological analysis of electron density may be classified as noncovalent and partly covalent closed-shell interactions. Values of the interactions energies confirms that the main contribute to adsorption energy receives from hydrogen bonds. Electron attaching reflects in increasing of binding between **CL-20** and silica surface due to stronger hydrogen bonds formation. Analysis of such parameters as electron affinity, ionization potential, reduction Gibbs free energy, oxidation Gibbs free energy, reduction and oxidation potentials shows that adsorbed **CL-20** is more resistant to oxidation and reduction processes as compared with hydrated species. Thus, adsorption may retard of the beginning of abiotic and biotic decomposition and decrease of the degradation rate of **CL-20** in soil.

Bibliography

[1] Sviatenko L. K. Are the reduction and oxidation properties of nitrocompounds dissolved in water different from those produced when adsorbed on a silica surface? An DFT M05-2X computational study / L. K. Sviatenko, O. Isayev, L. Gorb, F. C. Hill, D. Leszczynska, J. Leszczynski // J. Comput. Chem. – 2015. – Vol. 36, N 14. – P. 1029–1035.

[2] Sviatenko L. K. ANTA structure and redox properties of 5-amino-3-nitro-1H-1,2,4-triazole (ANTA) adsorbed on a silica surface: A DFT M05 computational study / L. K. Sviatenko, L. Gorb, F. C. Hill, D. Leszczynska, J. Leszczynski // J. Phys. Chem. A. – 2015. – Vol. 119, N 29. – P. 8139–8145.

[3] Robidoux P. Y. Acute and chronic toxicity of the new explosive CL-20 to the earthworm (Eisenia andrei) exposed to amended natural soils / P. Y. Robidoux, G. I. Sunahara, K. Savard, Y. Berthelot, S. Dodard, M. Martel, P. Gong, J. Hawari// Environ. Toxicol. Chem. – 2004. – Vol. 23. – P. 1026–1034.

[4] Kuperman R. G. Environmental Fate and Transport of a New Energetic Material CL-20. SERDP Report ER-1254/ R. G. Kuperman, R. T. Checkai, M. Simini. – U.S. Army Edgewood Chemical Biological Center, 2006.

[5] Gaussian 09, Revision A.02 / M. J. Frisch, G. W. Trucks, H. B. Schlegel, et al. – Gaussian, Inc.: Wallingford CT, 2009.

[6] Head-Gordon M. MP2 energy evaluation by direct methods / M. Head-Gordon, J. A. Pople, M. J. Frisch // Chem. Phys. Lett. – 1988. – Vol. 153. – P. 503–506.

[7] Weigend F. Balanced basis sets of split valence, triple zeta valence and quadruple zeta valence quality for H to Rn: Design and assessment of accuracy / F. Weigend, R. Ahlrichs // Phys. Chem. Chem. Phys. – 2005. – Vol. 7. – P. 3297–3305.

[8] Sviatenko L. K. Toward robust computational electrochemical predicting the environmental fate of organic pollutants / L. K. Sviatenko, O. Isayev, L. Gorb, F. Hill, J. Leszczynski // J. Comput. Chem. – 2011. – Vol. 32. – P. 2195–2203.

[9] Kihara K. An X-ray study of the temperature dependence of the quartz structure // Eur. J. Mineral. – 1990. – Vol. 2. – P. 63–77.

[10] Scott A. M. Theoretical study of adsorption of nitrogen-containing environmental contaminants on kaolinite surfaces / A. M. Scott, E. A. Burns, F. C. Hill // J. Mol. Model. – 2014. – Vol. 20. – P. 2373–2377.

[11] Bader R. W. F. Atoms in Molecules. A Quantum Theory / R. W. F. Bader. – Oxford: Calendon Press, 1990.

[12] Lu T. Multiwfn: A multifunctional wavefunction analyzer / T. Lu, F. Chen // J. Comput. Chem. – 2012. – Vol. 33, N 5. – P. 580–592.

[13] Cossi M. New developments in the polarizable continuum model for quantum mechanical and classical calculations on molecules in solution / M. Cossi, G. Scalmani, N. Rega, V. Barone // J. Chem. Phys. – 2002. – Vol. 117. – P. 43–54.

[14] Marenich A. V. Universal solvation model based on solute electron density and on a continuum model of the solvent defined by the bulk dielectric constant and atomic surface tensions / A. V. Marenich, C. J. Cramer, D. G. Truhlar // J. Phys. Chem. B – 2009. – Vol. 113. – P. 6378–6396.

[15] Kholod Y. An analysis of stable forms of CL-20: A DFT study of conformational transitions, infrared and Raman spectra / Y. Kholod, S. Okovytyy, G. Kuramshina, M. Qasim, L. Gorb, J. Leszczynski // J. Mol. Struct. – 2007. – Vol. 843. – P. 14–25.

[16] Molt R. W. Jr. Conformers of CL-20 Explosive and ab Initio Refinement Using Perturbation Theory: Implications to Detonation Mechanisms / R. W. Jr. Molt, R. J. Bartlett, T. Jr. Watson, A. P. Bazante // J. Phys. Chem. A – 2012. – Vol. 116. – P. 12129–12135.

[17] Mata I. Universal Features of the Electron Density Distribution in Hydrogen-Bonding Regions: A Comprehensive Study Involving H···X (X=H, C, N, O, F, S, Cl, P) Interactions / I. Mata, I. Alkorta, E. Molins, E. Espinosa // Chem. Eur. J. – 2010. – Vol. 16. – 2442–2452.

[18] Cremer D. A description of the chemical bond in terms of local properties of electron density and energy / D. Cremer, E. Kraka // Croat. Chem. Acta – 1984. – Vol. 57, N 6. – P. 1259–1281.

[19] Bader R. F. W. The characterization of atomic interactions / R. F. W. Bader, H. Essen // J. Chem. Phys. – 1984. – Vol. 80, N 5. – P. 1943–1960.

[20] Koch U. Characterization of C-H-O Hydrogen Bonds on the Basis of the Charge Density / U. Koch, P. L. A. Popelier // J. Phys. Chem. – 1995. – Vol. 99. – P. 9747–9754.

[21] Tang T.-H. Hydrogen bonds: relation between lengths and electron densities at bond critical points / T.-H. Tang, E. Deretey, S. J. Knak Jensen, I. G. Csizmadia // Eur. Phys. J. D – 2006. – Vol. 37. – P. 217–222.

[22] Pourbaix M. Atlas of electrochemical equilibria in aqueous solutions / M. Pourbaix. – 2nd ed. – Houston: National Association of Corrosion Engineers, 1974. – 644 p.

[23] Balakrishnan V. K. Decomposition of the Polycyclic Nitramine Explosive, CL-20, by Fe^0 / V. K. Balakrishnan, F. Monteil-Rivera, A. Halasz, A. Corbeanu, J. Hawari // Environ. Sci. Technol. – 2004. – Vol. 38. – P. 6861–6866.

[24] Uchimiya M. One-electron standard reduction potentials of nitroaromatic and cyclic nitramine explosives / M. Uchimiya, L. Gorb, O. Isayev, M. M. Qasim, J. Leszczynski // Environ Pollut. – 2010. – Vol. 158. – P. 3048–3053.

References

[1] Sviatenko, L. K., Isayev, O., Gorb, L., Hill, F. C., Leszczynska, D., & Leszczynski, J. (2015). Are the reduction and oxidation properties of nitrocompounds dissolved in water different from those produced when adsorbed on a silica surface? An DFT M05-2X computational study. *J. Comput. Chem.*, *36*(14), 1029–1035.

[2] Sviatenko, L. K., Gorb, L., Hill, F. C., Leszczynska, D., & Leszczynski, J. (2015). ANTA structure and redox properties of 5-amino-3-nitro-1H-1,2,4-triazole (ANTA) adsorbed on a silica surface: A DFT M05 computational study. *J. Phys. Chem. A.*, *119*(29), 8139–8145.

[3] Robidoux, P. Y., Sunahara, G. I., Savard, K., Berthelot, Y., Dodard, S., Martel, M., Gong, P., & Hawari, J. (2004). Acute and chronic toxicity of the new explosive CL-20 to the earthworm (Eisenia andrei) exposed to amended natural soils. *Environ. Toxicol. Chem.*, *23*, 1026–1034.

[4] Kuperman, R. G., Checkai, R. T., & Simini, M. (2006). Environmental Fate and Transport of a New Energetic Material CL-20. U.S. Army Edgewood Chemical Biological Center, SERDP Report ER-1254.

[5] Frisch, M. J., Trucks, G. W., Schlegel, H. B., Scuseria, G. E., Robb, M. A., Cheeseman, J. R., Scalmani, G., Barone, V., Mennucci, B., Petersson, G. A., Nakatsuji, H., Caricato, M., Li, X., Hratchian, H. P., Izmaylov, A. F., Bloino, J., Zheng, G., Sonnenberg, J. L., Hada, M., Ehara, M., Toyota, K., Fukuda, R., Hasegawa, J., Ishida, M., Nakajima, T., Honda, Y., Kitao, O., Nakai, H., Vreven, T., Montgomery, Jr. J. A., Peralta, J. E., Ogliaro, F., Bearpark, M., Heyd, J. J., Brothers, E., Kudin, K. N., Staroverov, V. N., Kobayashi, R., Normand, J., Raghavachari, K., Rendell, A., Burant, J. C., Iyengar, S. S., Tomasi, J., Cossi, M., Rega, N., Millam, J. M., Klene, M., Knox, J. E., Cross, J. B., Bakken, V., Adamo, C., Jaramillo, J., Gomperts, R., Stratmann, R. E., Yazyev, O., Austin, A. J., Cammi, R., Pomelli, C., Ochterski, J. W., Martin, R. L., Morokuma, K., Zakrzewski, V. G., Voth, G. A., Salvador, P., Dannenberg, J. J., Dapprich, S., Daniels, A. D., Farkas, Ö., Foresman, J. B., Ortiz, J. V., Cioslowski, J., & Fox, D. J. (2009). Gaussian 09 (Revision A.02) [Computer software]. Gaussian Inc., Wallingford CT.

[6] Head-Gordon, M., Pople, J. A., & Frisch, M. J. (1988). MP2 energy evaluation by direct methods. *Chem. Phys. Lett.*, *153*, 503–506.

[7] Weigend, F., & Ahlrichs, R. (2005). Balanced basis sets of split valence, triple zeta valence and quadruple zeta valence quality for H to Rn: Design and assessment of accuracy. *Phys. Chem. Chem. Phys.*, *7*, 3297–3305.

[8] Sviatenko, L., Isayev, O., Gorb, L., Hill, F., & Leszczynski, J. (2011). Toward robust computational electrochemical predicting the environmental fate of organic pollutants. *J. Comput. Chem.*, *32*, 2195–2203.

[9] Kihara, K. (1990). An X-ray study of the temperature dependence of the quartz structure. *Eur. J. Mineral.*, *2*, 63–77.

[10] Michalkova Scott, A., Burns, E. A., & Hill, F. C. (2014). Theoretical study of adsorption of nitrogen-containing environmental contaminants on kaolinite surfaces. *J. Mol. Model.*, *20*, 2373–2377.

[11] Bader, R. W. F. (1990). *Atoms in Molecules. A Quantum Theory.* Oxford, UK: Calendon Press.

[12] Lu, T., & Chen, F. (2012). Multiwfn: A multifunctional wavefunction analyzer. *J. Comput. Chem.*, *33*(5), 580–592.

[13] Cossi, M., Scalmani, G., Rega, N., & Barone, V. (2002). New developments in the polarizable continuum model for quantum mechanical and classical calculations on molecules in solution. *J. Chem. Phys.*, *117*, 43–54.

[14] Marenich, A. V., Cramer, C. J., & Truhlar, D. G. (2009). Universal solvation model based on solute electron density and on a continuum model of the solvent defined by the bulk dielectric constant and atomic surface tensions. *J. Phys. Chem. B*, *113*, 6378–6396.

[15] Kholod, Y., Okovytyy, S., Kuramshina, G., Qasim, M., Gorb, L., & Leszczynski, J. (2007). An analysis of stable forms of CL-20: A DFT study of conformational transitions, infrared and Raman spectra. *J. Mol. Struct.*, *843*, 14–25.

[16] Molt, R. W. Jr., Bartlett, R. J., Watson, T. Jr., & Bazante, A. P. (2012). Conformers of CL-20 Explosive and ab Initio Refinement Using Perturbation Theory: Implications to Detonation Mechanisms. *J. Phys. Chem. A*, *116*, 12129–12135.

[17] Mata, I., Alkorta, I., Molins, E., & Espinosa, E. (2010). Universal Features of the Electron Density Distribution in Hydrogen-Bonding Regions: A Comprehensive Study Involving H···X (X=H, C, N, O, F, S, Cl, p) Interactions. *Chem. Eur. J.*, *16*, 2442–2452.

[18] Cremer, D., & Kraka, E. (1984). A description of the chemical bond in terms of local properties of electron density and energy. *Croat. Chem. Acta*, *57*(6), 1259–1281.

[19] Bader, R. F. W., & Essen, H. (1984). The characterization of atomic interactions. *J. Chem. Phys.*, *80*(5), 1943–1960.

[20] Koch, U., & Popelier, P. L. A. (1995). Characterization of C-H-O Hydrogen Bonds on the Basis of the Charge Density. *J. Phys. Chem.*, *99*, 9747–9754.

[21] Tang, T.-H., Deretey, E., Knak Jensen, S. J., & Csizmadia, I. G. (2006). Hydrogen bonds: relation between lengths and electron densities at bond critical points. *Eur. Phys. J. D*, *37*, 217–222.

[22] Pourbaix, M. (1974). *Atlas of Electrochemical Equilibria in Aqueous Solutions* (2nd ed.). National Association of Corrosion Engineers: Houston.

[23] Balakrishnan, V. K., Monteil-Rivera, F., Halasz, A., Corbeanu, A., & Hawari, J. (2004). Decomposition of the Polycyclic Nitramine Explosive, CL-20, by Fe^0. Environ. *Sci. Technol.*, *38*, 6861–6866.

[24] Uchimiya, M., Gorb, L., Isayev, O., Qasim, M. M., & Leszczynski, J. (2010). One-electron standard reduction potentials of nitroaromatic and cyclic nitramine explosives. *Environ Pollut.*, *158*, 3048–3053.